DOI: 10.35595/2414-9179-2020-3-26-271-285

Mirzoolim A. Avliyakulov[1], Mamta Kumari[2], Nurmamat Q. Rajabov[3], Normat Kh. Durdiev[4]

CHARACTERIZATION OF SOIL SALINITY AND ITS IMPACT ON WHEAT CROP USING SPACE-BORNE HYPERSPECTRAL DATA

ABSTRACT

Facing the risk of soil salinization worldwide, there has been a growing interest in identifying rapid and inexpensive tools for soil salinity assessment. Remote sensing has shown great advantages in the field in recent decades. In present research, Hyperion Hyperspectral remote sensing data (EO-1) was used for characterization and mapping of salt-affected soils, to generate crop inventory map and to evaluate soil salinity impact on wheat crop growth in part of Mathura district of Uttar Pradesh representing Indo-Gangetic plain. Narrow bands can discriminate critical spectral differentials in detail and can assess the salinity hazard over crop. A detailed field survey was carried out in the study area in order to identify the salt-affected soils and to collect soil samples, groundwater table depth, chlorophyll content, LAI to characterize impact of soil salinity over crop. Various wheat crop spectra were collected for calculation of narrow band indices to discriminate various stress conditions. Spectral angle mapper (SAM) was used to generate crop inventory map with various types of crops. The same technique (SAM) was used to map various categories of salt affected soils represented by spectral endmembers of normal, slightly, moderately and highly salt-affected soils. The results showed that various severity classes of salt-affected soils could be reliably mapped using spectral angle mapper (SAM) analysis with an overall accuracy of 74.24%. Empirical relationships developed between crop & soil parameters and vegetation indices using SMLR could show its possibility with an R^2 of 0.52 and 0.41 to predict LAI and CCI, respectively. Validation results showed the RMSE of 0.8 and 5.2 to predict LAI and CCI. Partial least square regression (PLSR) statistical model (using spectroradiometer derived narrow band indices) was developed to assess different stress level with varying crop and soil parameters.

KEYWORDS: hyperspectral data, salinity mapping, SAM, PLSR, SMLR

INTRODUCTION

Soil salinity is major soil quality indicators in arid and semi-arid area which adversely affect plant growth and development. Salinization is one of the most common land degradation processes and a severe environmental hazard [*Dehaan, Taylor*, 2002; 2003; *Metternicht, Zinck*, 2003]. The salt in the soil solution (the "osmotic stress") reduces leaf growth and to a lesser extent root growth, and decreases stomatal conductance and thereby photosynthesis [*Munns*, 1993]. Soil salinization influences soil properties, leading to reduction in crop yields and land productivity. Basically, soil salinity is a dynamic process with severe consequences for the soil, hydrological, climatic, edaphic, geochemical, agricultural, social, and economic aspects. Therefore, for greater development and implementation of sufficient soil reclamation programs and preventing any further salinization to sustain agricultural lands and natural ecosystems, information on the spatial extent, nature and distribution of soil salinity is becoming very essential. Thus, timely detection of soil salinity, monitoring and assessment of its severity level and extent become very important in

[1] Cotton Breeding, Seed Production and Agrotechnologies Research Institute (CBSPARI), P.O. Box 111202, UzPITI str., Tashkent province, Uzbekistan; *e-mail*: **mirzoolim89@gmail.com**
[2] Indian Institute of Remote Sensing (IIRS), Kalidas road str., 4, Dehradun, India; *e-mail:* **mamta9507@gmail.com**
[3] Tashkent Institute of Irrigation and Agricultural Mechanization Engineers (TIIAME), P.O. Box 100000, Kori-Niyoziy str., 39, Tashkent, Uzbekistan; *e-mail*: **tiqxmmi1977@mail.ru**
[4] Cotton Breeding, Seed Production and Agrotechnologies Research Institute (CBSPARI), P.O. Box 111202, UzPITI str., Tashkent province, Uzbekistan; *e-mail*: **normat8689@mail.ru**

its beginning at local and regional scales. A large area of the Indo-Gangetic plain including Uttar Pradesh state consists of irrigated command area of arid and semi-arid climatic conditions and these areas are facing serious threats of land degradation due to salinization and alkalinization. Nearly 3.37 % of total geographical area of Mathura district is characterized under wasteland category and of which 26.46 % area is affected by salinity and alkalinity (http:/dolr.nic.in/wasteland.htm). Expansion of irrigation for intensive agriculture in this region has led to the development of salt-affected soils (FAO 1983) and poses significant threat to the world's productive capacity of soil and food grain production. Salinization and alkalization induced soil degradation occur in irrigated area where the water table approaches to the ground surface. Salts lying below sub-surface soil layer get dissolved and transported to the surface and sub-surface soils and adversely affect physio-chemical properties of these soils. It causes reduction in soil fertility and its productivity. Therefore, a reliable information on the nature and spatial extent of various severity classes of salt-affected soils are prerequisite to restore their fertility and to prevent their further degradation [*Ghosh et al.*, 2012].

Facing the risk of soil salinization worldwide, there has been a growing interest in identifying rapid and inexpensive tools for soil salinity assessment [*Metternicht, Zinck*, 2003]. Remote sensing has shown great advantages in the field in recent decades. As a remotely sensed indicator, the type and growing conditions of vegetation can provide a spatial overview of salinity distribution [*Dehaan, Taylor,* 2002; *Tilley et al.,* 2007; *Zhang et al.,* 1997], which thus help land managers to reduce the risk of salinization [*Wiegand et al.,* 1994]. Soil salinity can be detected directly from remotely sensed data through salt features that are visible at the soil surface, such as bare soil with white salt crusts on the surface or indirectly from indicators such as the presence of halophytic plant, the performance level of salt-tolerant crops [*Allbed, Kumar*, 2013]. Salt-affected soils are formed as accumulation of salts in the surface and sub-surface of soil and develop surface features that help in mapping their spatial extent and severities. Identification of these soil surface features serves as useful input for assessing salt affected soils. As salinity increases, more salts will appear at the soil surface, favoring the use of conventional remote sensing tools. In general, reflectance increases with increase in salt concentration on the surface of soil [*Ghosh et al.*, 2012]. Soil salinity is the dynamic process leading to constraints in identification of proper behavior of salt features, spectrally, spatially and temporally. Detection of salts on the surface can be difficult due to the presence of vegetation and other surface features that may contribute to creating spectral confusion with the salt reflectance properties. In this domain, the spectral bands most sensitive to salt-stress across diverse plants have not yet been defined; therefore, the predictive ability of previous vegetation indices (VIs) may not be satisfied for salinization monitoring. The soil samples and crop spectra were collected to investigate the relationship between vegetation spectra and soil salinity in part of Mathura district of irrigation command area of Indo-Gangetic Alluvial plains.

Mapping and monitoring soil salinity using remote sensing data has advantages. Using remote sensing technology include saving time, wide coverage (satellite remote sensing data provides the only source when data is required over large areas or regions), are faster than ground methods, and facilitate long term monitoring. These techniques provide multispectral image with resolutions that can be ranged from medium to high, as well as Hyperspectral image. These remotely sensed data have been successfully used for monitoring and mapping soil salinity for decades with mixed results. Many researchers have used different techniques to monitor and map soil salinity using remote sensing data, as discussed below.

Extensive research using satellite imagery for mapping and monitoring soil salinity has been conducted over the last three decades, mostly with multispectral sensors. These include Landsat Thematic Mapper (TM), Landsat Multispectral Scanner System (MSS), Landsat Enhanced Thematic Mapper Plus (ETM+), SPOT, Advanced Spaceborne Thermal Emission and Reflection Radiometer (Terra-ASTER), Linear imaging self-scanning sensor (LISS-III, LISS IV) and IKONOS [*Verma et al.,* 1994; *Dwivedi,* 2001; *Dwivedi,* 2008]. Application of broadband remote sensing in salinity studies is restricted due to limitations in spatial and especially spectral resolution that masks detailed of various kinds of salt-affected lands spectral signatures [*Cloutis,* 1996]. A variety of image processing methods such as supervised classification and spectral extraction techniques were used in the past to extract information from these multispectral satellite data in mapping of salt-affected soils [*Verma et al.*, 1994; *Dwivedi, Sreenivas,* 1998; *Metternicht, Zinck,* 2003; *Howari*, 2003]. However, it is very difficult to distinguish the degree of salinity using broadband multispectral data as there is spectral confusion. Through multispectral data it can be discriminated only saline and non-saline classes of soil. There can be observed spectral confusion between classes of moderately, slightly salt-affected soils and normal soils. Some studies [*Peng,* 1998]; used geographic information system techniques to integrate multispectral data with field data, such as groundwater mineralization, groundwater depth, and topographic data, to overcome the weakness of multispectral images. They were successful in mapping salinity classes, but required ground measurements in numerous training areas and could not quantitatively estimate soil salinity.

Hyperspectral sensors are a powerful and versatile tool for monitoring environmental stress because of the continuous sampling and the high spectral resolution. Narrow bands can discriminate critical spectral differentials in detail and can assess the salinity hazard over crop. Furthermore, hyperspectral remote sensing data provide almost continuous reflectance spectrum and help to generate unique spectral signature of various surfaces to map them with high accuracy. Various Image processing methods such as spectral unmixing technique, the linear mixture model (LMM) were used for characterization and mapping salt affected soils. Various categories of salt affected soil represented as endmembers are used for spectral unmixing analysis [*Tompkins et al.,* 1997; *Ghosh et al.*, 2012]. Potential of hyperspectral satellite data in mapping of salt-affected soils were investigated by several researchers [*Dehaan, Taylor*, 2002; *Taylor, Dehaan,* 2003; *Dutkiewicz et al.,* 2009].

Recently, several hyperspectral indices such as brightness index (BI), salinity index (SI), saturation index (SI) and hue index (HI) were successfully used for quantitative mapping salt affected soils, SOC and SOM using hyperspectral satellite data (Hyperion) [*Zhuo et al.,* 2008]. The spectral reflectance of the salt features at the soil surface has been widely studied using remote sensing and used as a direct indicator for soil salinity detection and mapping. However, when the soil moisture is high or the crust salt is invisible on the soil surface or mixed with other soil constituents, this direct approach becomes complicated and may yield unreliable results since these factors influence the soil spectral reflectance. On the basis of this concept, the simple ratio, SR [*Jordan,* 1969], the normalized difference vegetation index, NDVI [*Rouse et al.,* 1974], the enhanced vegetation index, EVI [*Huete et al.,* 1996.], the green atmospherically resistant vegetation index, GARI [*Gitelson et al.,* 1996] and etc. are used to assess the impact of soil salinity over crop growth.

In recent years, several multivariate statistical techniques such as partial least square regression (PLSR), stepwise multiple linear regression (SMLR) have been used to develop the relationship between soil and crop parameters as well as field derived spectra for assessing the impact of soil salinity over crop growth. PLSR is one of the most common methods for analysis spectral data for spectral calibration and prediction. In recent years, PLSR has been used to build LAI and CCI prediction models [*Madari et al.*, 2006; *Stevens et al.*, 2006].

There are different techniques used for matching the measured spectra with reference spectra depending on the criteria adopted for measuring the similarity/ closeness between the two spectra. Broadly these techniques are distance-based, angle-based and correlation-based measure. Spectral Angle Mapper (SAM) is a physically-based spectral classification that uses an *n*-D angle to match pixels to reference spectra.

Spectral Angle Mapper mapping method was used to complete the objectives of the work which is given below:

- to prepare soil salinity map of study area using Hyperion data;
- to prepare the crop inventory map of study area using Hyperion data;
- to evaluate soil salinity impact on wheat crop using Hyperion data.

MATERIALS AND METHODS OF RESEARCHES

Study area

A part of Mathura district of Uttar Pradesh representing Indo-Gangetic plain was selected for the study. Mathura is one of the western districts of Uttar Pradesh and forms a part of Yamuna basin and lies between 26° 76′ to 27° 62′ North latitudes and 77° 31′ to 77° 59′ East longitude. The area has good network of irrigation canal, distributaries and minors to irrigate the field. The Mathura district is having a serious problem of salty, brackish, oily water, which is not suitable for irrigation.

The climate of the district is semi-arid and characterized by intense hot summers, cold and foggy winters and general dryness throughout the year except during south-west monsoon period from July to September.

The mean annual temperature is 24.4 °C, maximum temperature in May goes up to 45 °C and the minimum temperature dips up to 2° during winters. In winter season the mean maximum temperature is 23.8 °C in the first week of December and last week of February. The average annual rainfall varies between 505–620 mm and 92 % of it is received during the rainy season comprising July, August and September months of the year.

The year can be divided into three seasons for example winter season from December to February with January being the coldest months, summer season from March to middle of June being the hottest months. The rainy season which receives rains from South-West monsoon in July continues till the end of September followed by the post monsoon period from October to November.

The landscape of district is nearly level to very gentle sloping with moderate to poor surface drainage. Mathura district mostly consists of alluvial soils those are formed by the silt of Yamuna & Ganga canal, which are quite fertile whereas, the district is also having ravenous saline, alkaline and waterlogged soils. Soils developed in the district have been influenced by parent material and microclimate. Basically, the surface texture of soil ranges from silt loam to clay loam. In district the large area soils are immature, light sandy colour, coarse, silt loam to clay soils, low to medium salty with high concentration of water-soluble salts, medium calcareous, water logged with medium to high water holding capacity, medium carbonic matter nitrogen and parental/soil fertility, responsive to fertilizer use. These lands are intensively cultivated for wheat, rice, mustard, sugarcane, sorghum etc. crops.

Satellite Data used

- The Hyperion (EO-1) data corresponding to path and row number of 146/41 of Mathura district were acquired on May 15, 2005, and January 07, 2005. Hyperion has 242 contiguous spectral channels (22 bands with overlapped wavelengths) out of that 198 were calibrated and covering spectral range of 356–2576 nm at an interval of 10 nm. Bands 8 to 57 are for visible-to-near-infrared (VNIR) and 77 to 224 in shortwave-infrared (SWIR) regions [*Datt et al.*, 2003]. All 242 bands of Hyperion are not usable because of the increased signal to noise ratio. This increased noise relative to signal is the consequence of Hyperion's greater distance from the reflecting surface of the target and the increased atmospheric scattering and absorption that comes with space platform remote sensing [*Lillesand, Kiefer*, 2000]. The Level 1 radiometric (L1R) product was used in the study. According to sensor characteristics sensor spatial resolution is 30 m and 12 bit radiometric quantization [*Pearlman et al.*, 2003].
- IRS LISS IV data acquired on April 6, 2006 and Standard FCC at 1: 15 000 scale was generated for visual interpretation of salt affected soils, wheat crop condition and to locate these soils during field survey.
- Georeferenced Landsat ETM+ Data (Acquired on Oct. 22, 1999) was used to discriminate crops grown in the study area.
- During the generating of crop inventory map of the study area there were used multiple data to discriminate crops grown in area. January month 2005 Hyperion data was used for generating crop inventory map which is older data set. Real ground truth information 2014 might

not match with the year of 2005. Taking into account this fact it has been studied multiple datasets for discriminating of crops. As agronomy point of view, it is known every crop's length of growing period. As per this knowledge crops were identified in particular area for 2005.

Software's used

- ENVI 4.3, standard 5.0, (Environment for Visualizing Images, Research System, Inc) software was used for pre-processing and processing of the satellite data. It offers "Hyperion tool kit" to analyze Hyperspectral satellite data.
- ERDAS IMAGINE 13 was used to mask wheat area and accuracy assessment.
- ARC GIS 10.1 — developed by ESRI used to export generated maps.
- Statistical software: Statistica 7.0 is used for PLSR model.

Field data collection

A detailed field survey was carried out in the study area in order to identify the salt-affected soils and to collect soil samples (Theta probe), groundwater table depth, chlorophyll content (CCM 200), LAI (AccuPAR LP80) to characterize impact of soil salinity over crop vigour. Various wheat crop spectra were collected (SVC Spectroradiometer) with varying degree of salinity for calculation of narrow band indices to discriminate various stress conditions. Random sampling technique was applied and total 29 sites (3 additional highly salt affected lands) were identified where actual wheat crop field are selected for sample collection. Soil samples were collected from surface and subsurface of soil. Chlorophyll content was taken from the upper, middle and lower portion of wheat crop plant. LAI were taken upper side of crop (APAR), and below portion of canopy (BPAR). Crop biophysical parameters are taken in 4−5 repetitions for better accuracy. The surface and subsurface depth ranged from 0−15 and 15−30−40 cm. Thus, total of 58 samples (6 additional) were collected from the above-mentioned sites. Wheat crop spectra were collected with varying degree of salinity. The total number of crop spectra that was collected from SVC spectroradiometer was more than 130 (average four spectra for each of the locations) with various vegetation conditions of wheat crop. Soil samples were analyzed in laboratory to characterize pH, electrical conductivity (EC).

Pre-processing of Hyperion satellite data

Hyperion data was corrected for abnormal pixels, stripping affects prior to the atmospheric correction. In the study area, ENVI's Fast Line-of-sight Atmospheric Analysis of Spectral Hypercubes (FLAASH) module was applied on Hyperion data for atmospheric correction. The study area is rural and it falls in tropical climate. Thus, tropical atmospheric and rural aerosol model of FLAASH were selected and other parameters were defined based on metadata of the Hyperion image file.

Image endmembes were extracted following the standard processing steps of Minimum Noise Fraction (MNF) Transformation, Pixel Purity Index (PPI), Selection of Endmembers.

Accuracy assessment was performed to determine how accurately pixels were classified to various classes of the salt affected soils [*Janssen, Van der Wel*, 1994]. Performance of all classified maps was evaluated by accuracy assessment. Point map was prepared from optical images and used for performance evaluation. Confusion matrix was prepared to analyze accuracy of each agricultural class in crop inventory map and each soil salinity class in soil salinity map. Accuracy was estimated in reference to ground truth data for producer's, user's and overall accuracy. Kappa and kappa statistics were also calculated. Accuracy assessment was performed in ERDAS 13.

RESULTS OF RESEARCHES AND THEIR DISCUSSION

Physio-chemical characteristics of soils in the study area

The soil samples collected were air-dried to eliminate the influence of water content and passed through a 2-mm sieve to remove large debris, stones, and stubbles. The samples were analyzed for their physio-chemical properties. The surface and subsurface soil samples were analyzed for pH, EC, bulk density. The electrical conductivity (EC) was measured in extracted solutions using Electrical conductivity meter. Salt affected soils are in general categorized into slight, moderate and severe classes based on salt concentration in the soil.

Soil salinity map showing different levels of salinity has shown the maximum confusion between slightly salt affected and normal soil. An overall accuracy of 74.24 % was achieved. Crop inventory map showing different crops, land use and land cover features by the same mapping method SAM classifier has shown the overall accuracy of 82.14 % with a user's and producer's accuracy of 85 % for wheat class.

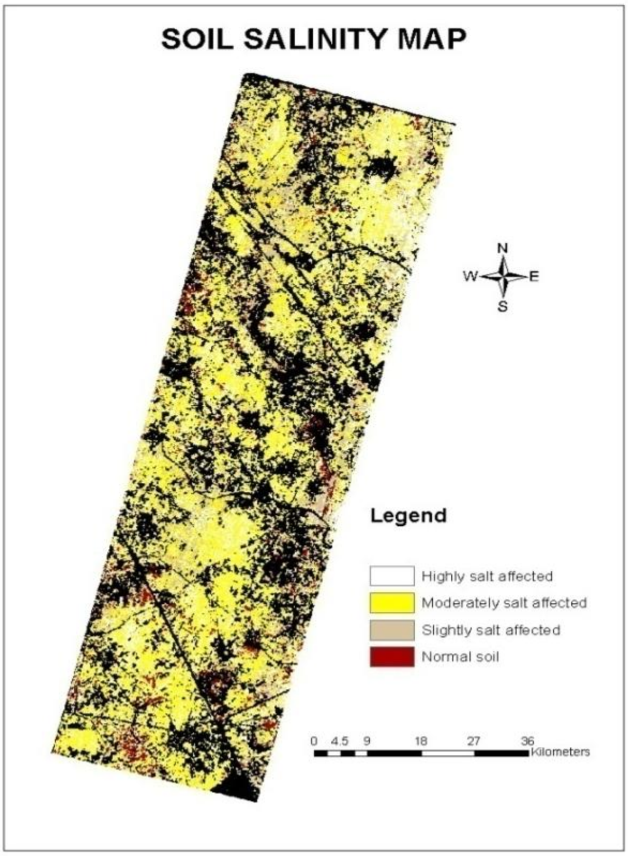

Fig. 1. Soil salinity map by using SAM mapping method

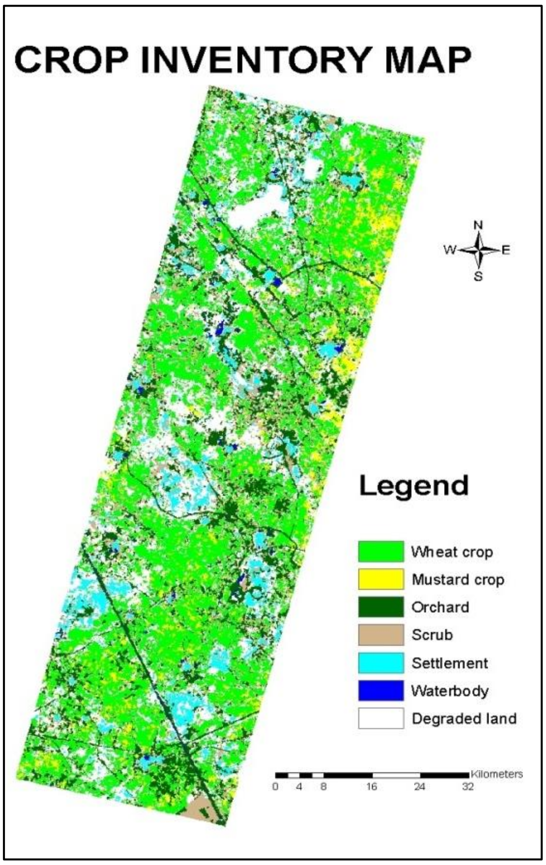

Fig. 2. Crop inventory map by using SAM mapping method

Indices to assess the soil salinity impact over crop growth

During the field investigation period more than 130 crop spectra were collected. From the field derived spectra 24 indices were calculated to evaluate the salinity impact over crop growth (table 1).

These indices were calculated from satellite image as well. After completing the preparation of crop inventory map the wheat area were extracted from the crop inventory map for further processing. Extracted wheat crop area was used to apply over indices map to see the impact of salinity over wheat crop vigour. Some results of indices are given below (fig. 3).

Among all 24 indices, modified red edge normalized difference vegetation index ($mNDVI_{705}$) and structure insensitive pigment index (SIPI) have shown efficiency to map the impact of soil salinity over wheat crop. However, both the indices behaved differently due to their different wavelength region and so its different response to target.

Table 1. Performance of vegetation indices for predicting soil salinity across wheat crop vigour with coefficient of determination (R^2) of linear regression

Vegetation indices	Formula
Modified red edge normalized difference vegetation index	$MNDVI_{705}$=750-705/750+705-2*445
Structure insensitive pigment index (SIPI)	SIPI=800-445/800-680
Normalized difference water index	NDWI=857-1241/857+1241
Enhanced vegetation index (EVI)	2.5 × (R800– R670)/(1 + R800+ 6 ×R670– 7.5 × R450)

The modified red edge normalized difference vegetation index (mNDVI $_{705}$) is a modification of the red edge NDVI. It differs from the red edge NDVI by incorporating a correction for leaf specular reflection. The mNDVI $_{705}$ capitalizes on the sensitivity of the vegetation red edge to small changes in canopy foliage content, gap fraction, and senescence. Applications include precision agriculture, forest monitoring, and vegetation stress detection.

The mNDVI $_{705}$ index is defined by the following equation:

$$mNDVI_{705}=750-705/750+705-2*445.$$

It can be understood from this formula that modified red edge NDVI mostly takes into account NIR reflectance. In fig. 3 (c) moderately and highly salt affected area crop condition is normal to moderately stressed. This can be explained by cell turgidity of plant. It is known that cell structure of plant is dominant factor in NIR region. Taking into account this fact NIR reflectance shows higher reflectance because of the cell turgidity. Proper irrigation can also reduce salinity hazard. It is not necessary that plant is not under any kind of stress. In contrast to mNDVI, SIPI has indicated some kind of stress due to less pigment (chlorophyll) content.

The structure insensitive pigment index (SIPI) is a reflectance measurement designed to maximize the sensitivity of the index to the ratio of bulk carotenoids (for example, alpha-carotene and beta-carotene) to chlorophyll while decreasing sensitivity to variation in canopy structure (i.e. LAI). Increases in SIPI are thought to indicate increased canopy stress (carotenoid pigment). Applications include vegetation health monitoring, plant physiological stress detection and crop production and yield analysis. SIPI is defined by the following equation:

$$SIPI=800-445/800-680.$$

In fig. 3 (b) structure intensive pigment index are taking into account leaf pigment and light use efficiency, because of this crop condition is varying between low vigour to moderate in high and moderately salt affected place.

The same tendency such as mNDVI can be seen in EVI and NDWI where NDWI are taking into account canopy water content of plant whereas EVI is one of the most common predictors of LAI. After calculation of all indices it has been selected 2 indices (mNDVI and SIPI) to evaluate salinity impact over wheat crop growth. In ENVI software matrix option has been selected to bring indices map and soil salinity map together to see and evaluate impact of salinity over crop growth. Here it can be seen by using matrix option classes are divided into 9 categories. These indicators show it can be seen that moderately salt affected places are stressed crops. The same explanation can be for highly salt affected areas also have normal crop condition this can be because of the proper irrigation, and agronomic management of crop.

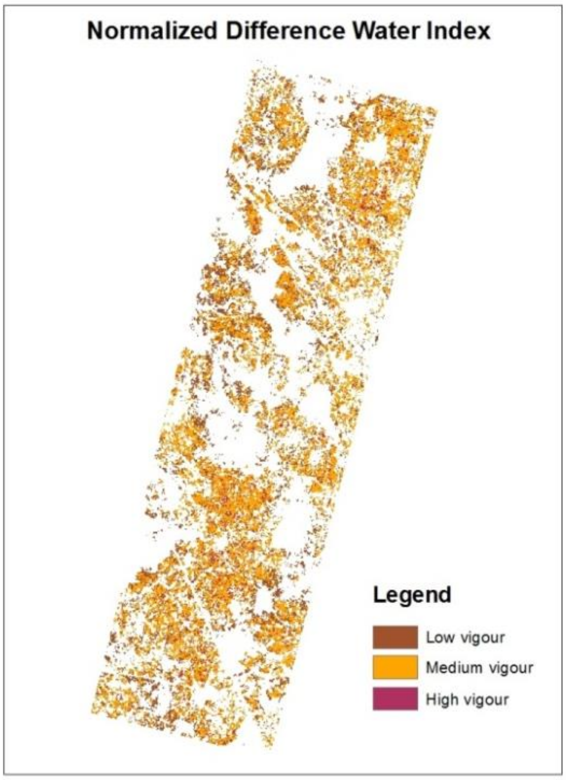

(a)

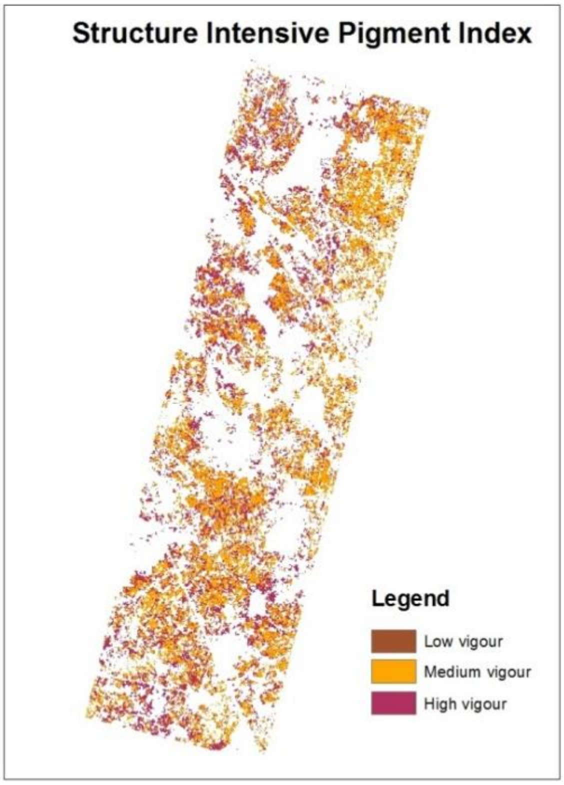

(b)

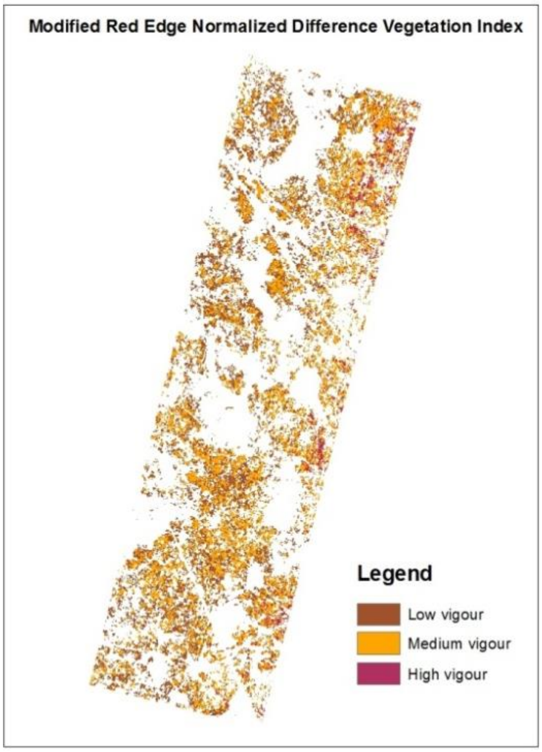

(c)

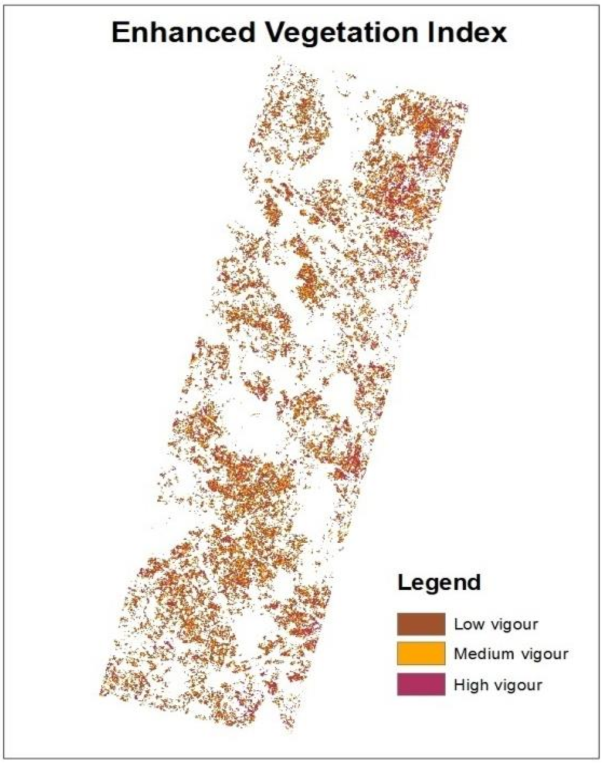

(d)

Fig. 3. Impact of salinity over wheat crop vigour (a) NDWI, (b) SIPI, (c) MRENDVI, (d) EVI

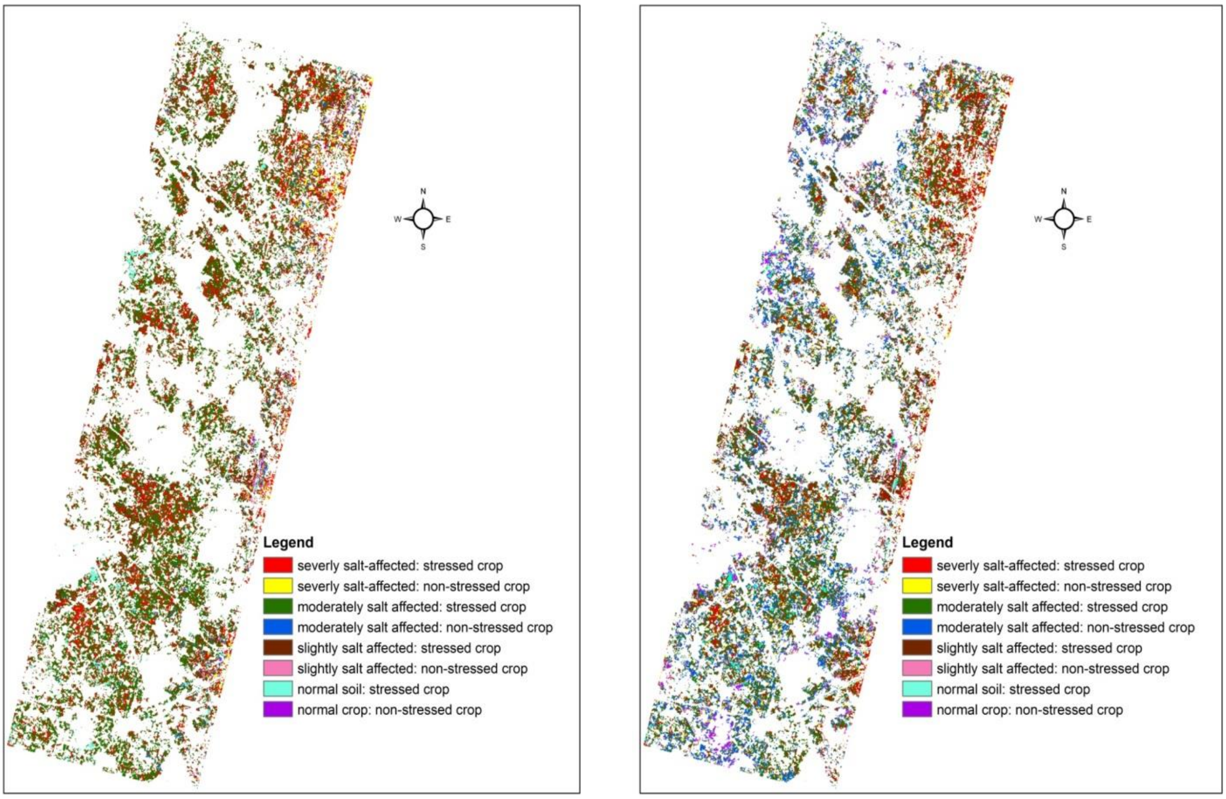

(a) *(b)*

Fig. 4. Impact of salinity over wheat crop:
(a) Salinity map: Modified Red Edge NDVI;
(b) Salinity map: Structure Intensive Pigment Index

Results of multivariate statistical techniques

Stepwise multiple linear regression (SMLR)

Empirical relationships developed between crop parameters (i.e., LAI and CCI) & soil parameters (i.e., pH and EC) and vegetation indices using Stepwise Multiple Linear Regression (SMLR) showed its fitness with an R^2 of 0.52 and 0.41 to predict LAI and CCI, respectively. Validation results showed the RMSE of 0.8 and 5.2 to predict LAI and CCI. Results of SMLR are given in table 2.

Table 2. Developed empirical relationships between crop and soil parameters and vegetation indices

Parameter	Empirical relationship	R^2
LAI	-10.12+10.45XWBI+4.98XEVI-87.49XNDLI-57.32XCAI+0.029XSR	0.52
CCI	-151.463 +71.21XmNDVI +78.53XMSI +84.63XWBI-0.153XSR	0.41
	-25.66XWBI+ 246.1X NDLI-4.3X EVI+16.65X mNDVI-0.05X CRI1+32.65XNDWI+14.73XMSI	0.40
	11.02-11.8XWBI-7.026X EVI+113.81X NDLI-0.03XCRI2+5.69XmNDVI	0.31
pH (Surface)	0.707+0.66XARI2+7.46XWBI+0.03XSR	0.16
	4.62+0.65xARI2+81.57XCAI-0.207XCRI2+5.34XWBI-5.93XNDWI-2.96XmNDVI-12.63XNDNI+3.2X EVI+0.20XCRI1	0.26

Validation of empirical relationships

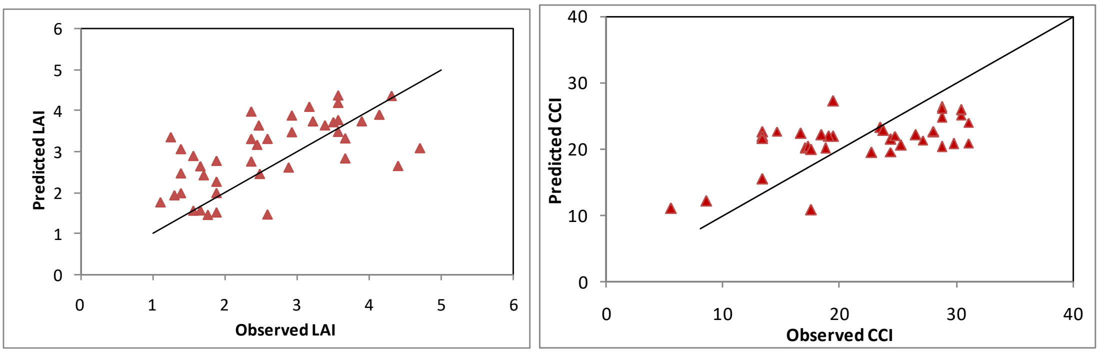

(a) (b)

Fig. 5. Validation graph of empirical relationship (a) LAI (b) CCI

Fig. 5 shows the validation of empirical relationships of predicted LAI and CCI. X axis of the graph shows the observed LAI and CCI which is dependant and ground-based factor where Y axis gives the information about predicted LAI and CCI and their relationship. Predicted LAI and CCI can be used to evaluate soil salinity impact over crop growth.

Table 3. Quantification of error of estimation

Parameter	RMSE	R^2
LAI	0.83	0.41
CCI	5.2	0.37

Partial least square regression (PLSR)

Using the Statistica 7.0 software, the relationship between crop parameters (i.e. LAI & CCI) and Soil parameter (i.e. EC and pH) and Hyperspectral indices were assessed using a Partial Least Squares (PLS) Regression.

A total of 24 spectral vegetation indices were calculated from reflectance responses. Indices represented each of the three main regions of the electromagnetic spectrum, i.e. VIS, NIR, and SWIR regions, each of which is associated with specific plant attributes, such as plant pigments, internal leaf structure and moisture content. Vegetation indices have been found to be related to plant biophysical properties, such as leaf area index, green cover, green biomass, or capacity of canopy to absorb photo-synthetically active radiation. To develop a multivariate relationship and to account for the multi-collinearity between indices PLSR has been performed between indices and the crop (i.e. LAI, CCI) and soil (i.e. EC) parameters. A separate test data has been used to validate the results.

Fig. 7 shows the relationship between LAI, CCI and EC with Hyperspectral indices. The indices contributing more information can be judged from its regression coefficients. The PLS regression results on the training data set demonstrated the potential to predict the LAI, CCI and EC from proximal hyperspectral data. There is a sufficient correlation between predicted and measured values for the validated samples, i.e. R2 of 0.61, 0.59 and 0.49 for LAI, CCI and EC respectively. The root means square error of prediction (RMSEP) was relatively low i.e. 0.7, 4.7 and 1.5 respectively indicates good forecast accuracy.

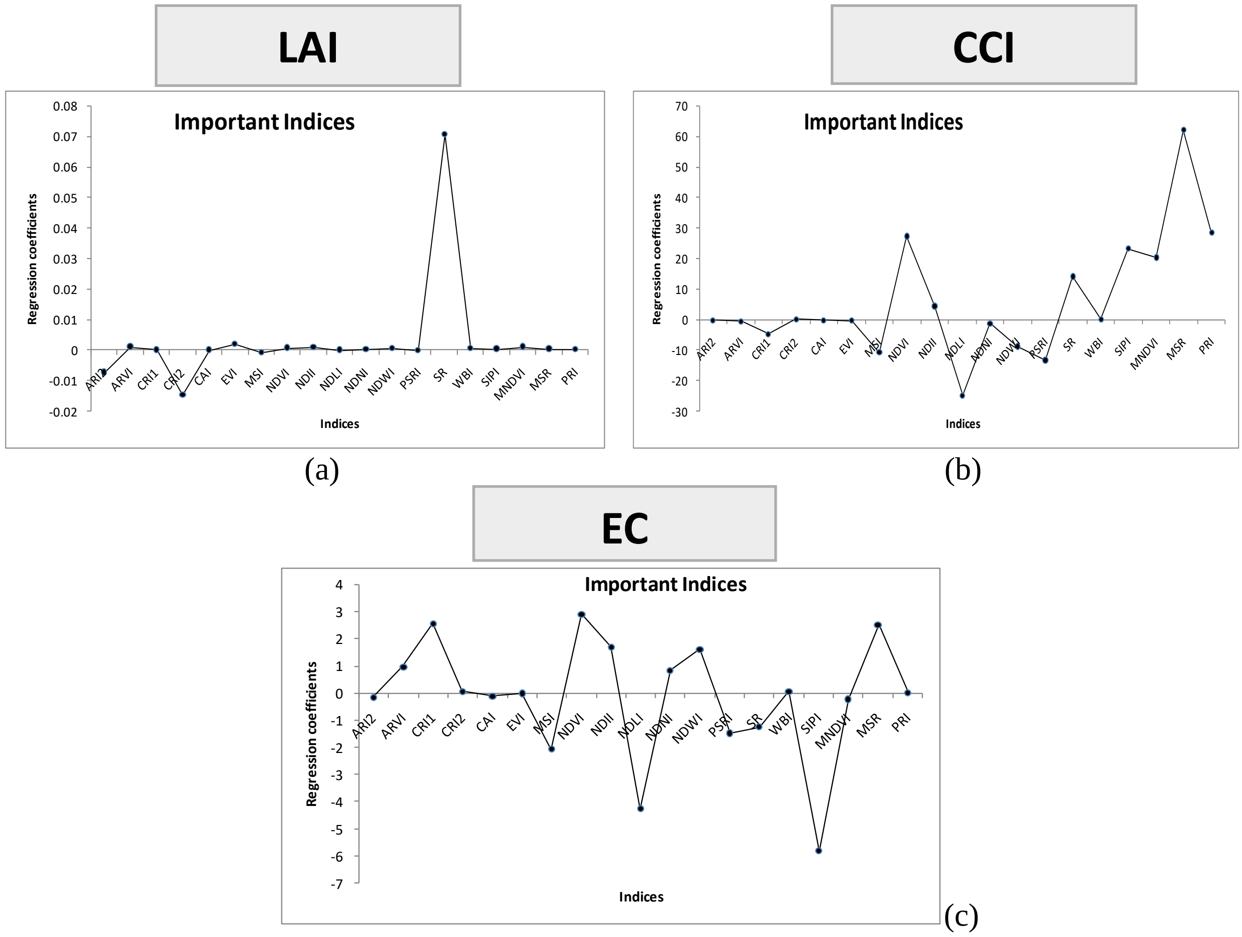

Fig. 6. Important indices related with ground-based parameter: (a) LAI, (b) CCI, (c) EC

Validation of PLSR model

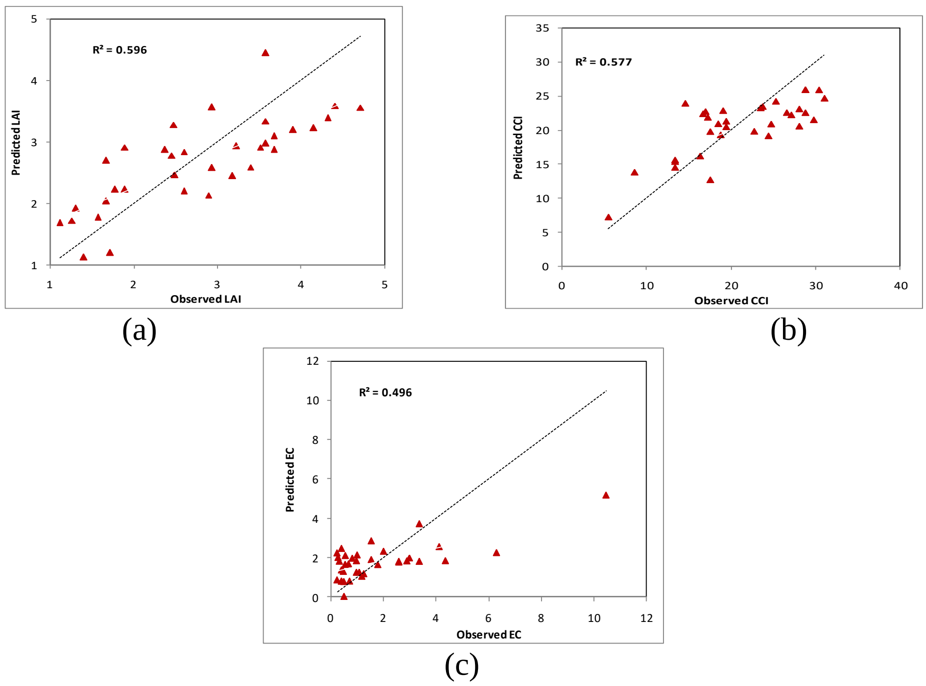

Fig. 7. Validation graph of PLSR model (a) LAI, (b) CCI, (c) EC

Table 4. Results of PLS regression of ground derived parameters and hyperspectral indices

Parameter	No of optimum No of PLS factor	RMSE	Important Indices
LAI	2	0.7	SR, CRI2, ARI2
CCI	7	4.7	MSR, PRI, NDVI, NDLI, MNDVI, SIPI
EC	5	1.5	CRI1, NDVI, NDLI, NDWI, SIPI, MSR

Predicted LAI and CCI

The predicted LAI and CCI map of year 2005 were produced by using stepwise multiple linear regression (SMLR) model (generated using year 2014 field data). The predicted map also showed the similar tendency to map crop stress status as that of individual vegetation indices.

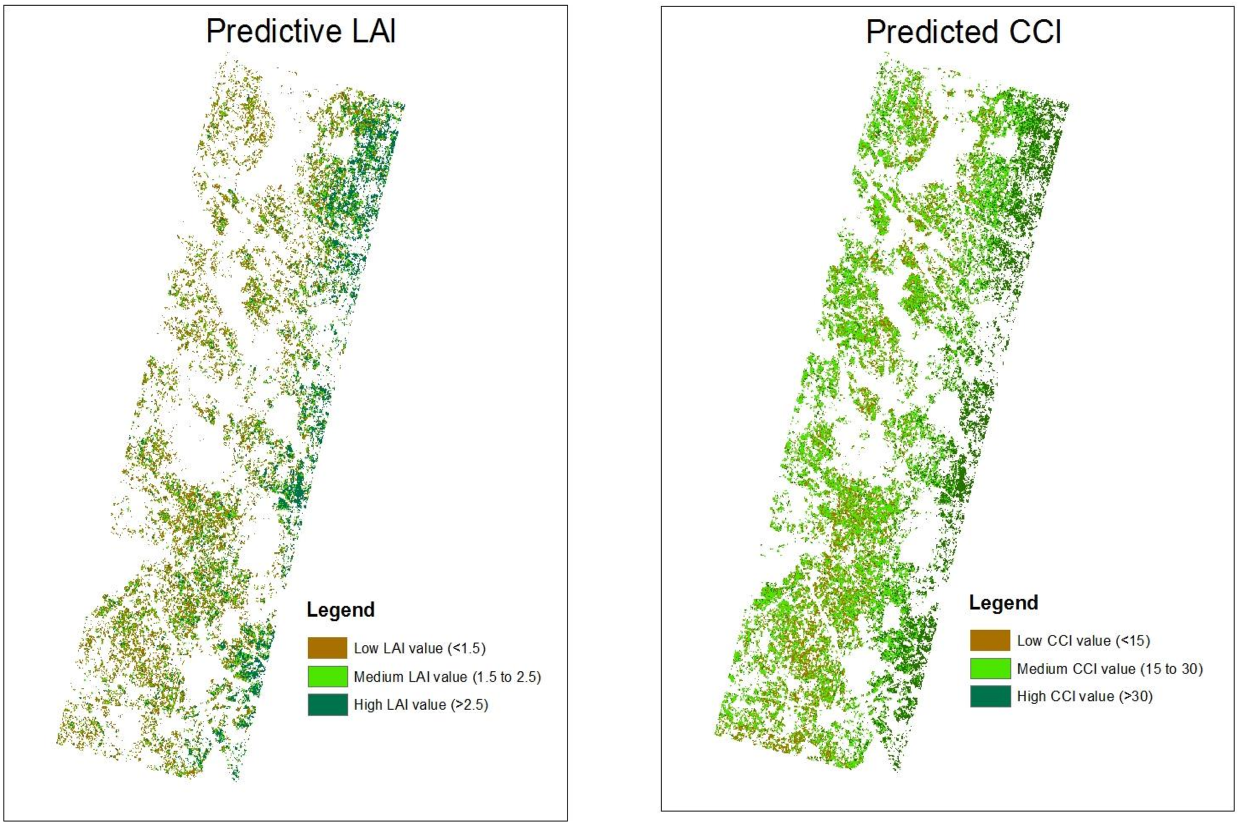

(a) (b)

Fig. 8. Predicted (a) LAI and (b) CCI maps (Jan, 2005) for crop stress assessment using SMLR statistical technique

After generating CCI and LAI maps density slicing operation has been done and classes were categorized having value low LAI (<1.5), medium LAI (1.5-2.5), high LAI (<2.5) whereas CCI values were low CCI (<15), medium CCI (15-30), high CCI (>30). The same tendency has been seen in LAI and CCI predicted maps as it is in indices.

CONCLUSIONS

Taking into consideration the data analyses, indices calculation, field data and statistical techniques it can be concluded and the following conclusions could be made from the results of this study:

Soil salinity map showing different levels of salinity by using spectral angle mapper mapping method has shown the maximum confusion between slightly salt affected and normal soil. An overall accuracy of 74.24 % was achieved.

The crop inventory map by the same mapping method SAM classifier has shown the overall accuracy of 82.14 % with a user's and producer's accuracy of 85 % for wheat class.

The narrow band and broad band vegetation indices could capture the variability of crop vigour with respect of soil salinity. While selecting each and every indice spectral region of the indices (VIS, NIR, SWIR), formula should be carefully considered in order to evaluate impact of soil salinity over crop growth. Results showed that mostly salt affected lands are having stressed crop but on the other hand some high vigour crops also can be seen in the affected land. This can be explained by agronomic point of view there can be proper irrigation facilities, management practices and also canopy cover will also play a role while calculating these indices.

Empirical relationships developed between crop biophysical parameters such as LAI and CCI and soil parameters (pH and EC) and vegetation indices using stepwise multiple linear regression (SMLR) multivariate statistical method could show its possibility with an R^2 of 0.52 and 0.41 to predict LAI and CCI, respectively. Validation results showed the RMSE of 0.8 and 5.2 to predict LAI and CCI.

Partial least square regression (PLSR) statistical technique by using Statistica 7.0 software regression results on the field data demonstrated the potential to predict the crop parameters (i.e. LAI and CCI) and soil parameter (i.e., EC). The predicted LAI and CCI map produced by SMLR also showed the similar tendency to map crop stress status as that of individual vegetation indices.

Finally, taking into account the fact that currently the major parts of soil of Mathura District of Uttar Pradesh are affected (26.46 %) by salinity and alkalinity. Remote sensing especially hyperspectral remote sensing with high spectral resolution can help to monitor and map salt affected areas with high accuracy which can help landowners, agronomists to manage better reclamation procedures. Therefore, at the expense of reducing mineralization and lowering the ground water levels on the irrigated lands can be prevented from the increase of moderately and highly salinization. Otherwise salt affected soils with various degree of salinity can adversely affect physico-chemical properties of soils which cause reduction in soil fertility and its productivity and it also negatively affects on plant growth and development. Complete system of desalinization of all types of soils has not been entirely investigated yet. This shows the importance of through comparative analyses of data, collected from research and investigations and generalizing working experience of leading landowners and farm associations. The solution to the problem is call of the times.

ACKNOWLEDGEMENTS

This publication is the part of the post graduate thesis. We gratefully acknowledge support under the UN CSSTEAP program conducted in Indian Institute of Remote Sensing (IIRS).

REFERENCES

1. *Abbas A., Khan Sh., Hussain N., Hanjra M.A., Akbar S.* Characterizing soil salinity in irrigated agriculture using a remote sensing approach. Physics and Chemistry of the Earth, 2013. No 55−57. P. 43–52.

2. *Aldakheel Y.Y.* Assessing NDVI spatial pattern as related to irrigation and soil salinity management in Al-Hassa Oasis, Saudi Arabia. Journal of the Indian Society of Remote Sensing, 2011. V. 39. No 2. P. 171−180. DOI: http://dx.doi.org/10.1007/s12524-010-0057-z.

3. *Allbed A., Kumar L.* Soil salinity mapping and monitoring in arid and semi-arid regions using remote sensing technology: A review. Advance in Remote Sensing Journal, 2013. No 2. P. 373−385. Web resource: http://www.scirp.org/journal/ars (accessed 12.12.2019).
4. *Boardman J.W., Kruse F.A.* Automated spectral analysis: A geologic example using AVIRIS data, north Grapevine Mountains, Nevada. Proceedings of Tenth Thematic Conference on Geologic Remote Sensing, Environmental Research Institute of Michigan, 1994. P. 407−418.
5. *Boardman J.W., Kruse F.A., Green R.O.* Mapping target signatures via partial unmixing of AVIRIS data. Summaries of Fifth JPL Airborne Earth Science workshop. JPL Publication, 1995. V. 1. P. 23−26.
6. *Cloutis E.A.* Hyperspectral geological remote sensing: Evaluation of analytical techniques. International Journal of Remote Sensing, 1996. No 17. P. 2215–2242.
7. *Datt B., Mcvicar T.R., Van Niel T.G., Jupp D.L.B., Pearlman J.S.* Preprocessing EO-1 Hyperion Hyperspectral data to support the application of agricultural indexes. IEEE Transaction in Geoscience and Remote Sensing, 2003. No 41 (6/1). P. 1246–1259.
8. *Dehaan R.L., Taylor G.R.* Field-derived spectra of salinized soils and vegetation as indicators of irrigation-induced soil salinization. Remote Sensing of Environment, 2002. No 80. P. 406–417.
9. *Dehaan R., Taylor G.R.* Image-derived spectral endmemders as indicators of salinization. International Journal of Remote Sensing, 2003. No 24. P. 775–794.
10. *Douaoui A.E.K., Hervé N., Walter Ch.* Detecting salinity hazards within a semiarid context by means of combining soil and remote-sensing data. Geoderma, 2006. No 134. P. 217–230.
11. *Dutkiewicz A., Lewis M., Ostendorf B.* Evaluation and comparison of hyperspectral imagery for mapping surface symptoms of dryland salinity. International Journal of Remote Sensing, 2009. No 30 (3). P. 693–719.
12. *Dwivedi R.S.* Soil resources mapping: A remote sensing perspective. Remote Sensing Reviews, 2001. V. 20. No 2. P. 89−122. DOI: http://dx.doi.org/10.1080/02757250109532430.
13. *Dwivedi R.S., Sreenivas K.* Image transforms as a tool for the study of soil salinity and alkalinity dynamics. International Journal of Remote Sensing, 1998. No 19. P. 605–619.
14. *Dwivedi R.S. et al.* 5 Generation of farm-level information on salt-affected soils using IKONOS-II multispec-tral data. Remote Sensing of Soil Salinization: Impact on Land Management. Boca Raton: CRC Press, 2008. DOI: http://dx.doi.org/10.1201/9781420065039.ch5.
15. *El-Nahry A.H., Hammad A.Y.* Assessment of salinity effects and vegetation stress, West of Suez Canal, Egypt using remote sensing techniques. Journal of Applied Sciences Research, 2009. No 5 (3). P. 316−322.
16. *Esbensen K.H.* Multivariate Data Analysis — in Practice. 5th edition. Norway, Oslo, 2002.
17. *Farifteh J., Farshad A., George R.J.* Assessing salt-affected soils using remote sensing, solute modelling, and geophysics. Geoderma, 2006. No 130. P. 191–206.
18. *Farifteh J., Van der Meera F., Atzbergerb C., Carranzaa E.J.M.* Quantitative analysis of salt-affected soil reflectance spectra: A comparison of two adaptive methods (PLSR and ANN). Remote Sensing of Environment, 2007. V. 110. No 1. P. 59−78.
19. *Ghosh G., Kumar S., Saha S.K.* Hyperspectral satellite data in mapping salt-affected soils using linear spectral unmixing analysis. Journal of the Indian Society of Remote Sensing, 2012. V. 40. No 1. P. 129−136.
20. *Gitelson A.A., Kaufman Y.J., Merzlyak M.N.* Use of a green channel in re-mote sensing of global vegetation from EOS-MODIS. Remote Sensing of Environment, 1996. No 58. P. 289–298.
21. Guidelines and evaluation for rainfed agriculture. Soil Bulletin, FAO, 1983. No 52.
22. *Howari F.M.* The use of remote sensing data to extract information from agricultural land with emphasis on soil salinity. Australian Journal Soil Res, 2003. No 41. P. 1243–1253.
23. *Huete A.R., Justice C., van Leeuwen W.* MODIS vegetation index (mod13). Algorithm theoretical basis document. Version 2. Greenbelt, Maryland 20771. USA: NASA Goddard Space Flight Center, 1996.

24. *Janssen*. Principle of Remote Sensing, International Institute for Aerospace survey and Earth Science. The Netherlands: ITC Enschede, 2001.
25. *Jordan C.F.* Derivation of leaf-area index from quality of light on forest floor. Ecology, 1969. No 50. P. 663.
26. *Lillesand T.M., Kiefer R.W.* Remote Sensing and Image Interpretation. 4th ed. Wiley & Sons, 2000.
27. *Madari B.E., Reeves Iii J.B., Machado P.L.O.A., Guimarães C.M., Torres E., McCarty G.W.* Mid- and near-infrared spectroscopic assessment of soil compositional parameters and structural indices in two Ferralsols. Geoderma, 2006. V. 136. No 1−2. P. 245−259.
28. *Mashimbye Z.E., Cho M.A., Nell J.P., Declercq W.P., Van Niekerk A., Turner D.P.* Model-based integrated methods for quantitative estimation of soil salinity from hyperspectral remote sensing data: A case study of selected South African soils. Soil Science Society of China, 2012. No 22 (5). P. 640–649.
29. *Metternicht G.I., Zinck J.A.* Remote sensing of soil salinity: potentials and constraints. Remote Sensing of Environment, 2003. No 85. P. 1–20.
30. *Metternicht G.I., Zinck J.A.* Spatial discrimination of salt- and sodium-affected soil surfaces. International Journal Remote Sensing, 1997. No 18. P. 2571–2586.
31. *Munns R.* Physiological processes limiting plant growth in saline soil: some dogmas and hypotheses. Plant Cell Environ, 1993. No 16. P. 15−24.
32. *Pearlman J.* Hyperion, a space-based imaging spectrometer. IEEE Transaction on Geoscience and Remote Sensing, 2003. No 41(6). P. 1160–1173.
33. *Peng W.* Synthetic analysis for extracting information on soil salinity using remote sensing and GIS: a case study of Yanggao basin in China. Environ. Manage, 1998. V. 22. P. 153–159.
34. *Rouse J.W., Haas R.H.Jr., Schell J.A., Deering D.W.* Monitoring vegetation systems in the Great Plains with ERTS. Third ERTS-1 Symposium, 1974. P. 309–317.
35. *Stevens A., Wesemael B., Vandenschrick G., Toure S., Tychon B.,* Detection of carbon stock change in agricultural soils using spectroscopic techniques. Soil Sci. Soc. Am. J., 2006. V. 70. P. 844−850.
36. *Tilley D.R., Ahmed M., Son J.H., Badrinarayanan H.* Hyperspectral reflectance response of freshwater macrophytes to salinity in a brackish subtropical marsh. Journal Environmental Quality, 2007. No 36. P. 780–789.
37. *Tompkins S., Mustard J.F., Pieters C.M., Forsyth D.W.* Optimization of endmembers for spectral mixture analysis. Remote Sensing of Environment, 1997. V. 59. P. 472–489.
38. *Verma K.S., Saxena R.K., Barthwal A.K., Deshmukh S.N.* Remote sensing technique for mapping salt affected soils. International Journal of Remote Sensing, 1994. V. 15. P. 1901–1914.
39. *Wiegand C.L., Rhoades J.D., Escobar D.E., Everitt J.H.* Photographic and video-graphic observations for determining and mapping the response of cotton to soil salinity. Remote Sens. Environ, 1994. V. 49. P. 212–223.
40. *Zhang M., Ustin S., Rejmankova E., Sanderson E.* Monitoring pacific coast salt marshes using remote sensing. Ecological Applications, 1997. No 7. P. 1039–1053.
41. *Zhuo L., Liu Y., Wu J., Wang J.* The international archives of photogrammetry. Remote Sensing and Spatial Information Sciences. Beijing, 2008. V. XXXVII. Part B8.